9454 *Macromolecules* **2010**, *43*, 9454–9461
DOI: 10.1021/ma101943k

Macromolecules
ARTICLE

# Supramolecular Structure of β-Cyclodextrin and Poly(ethylene oxide)-*block*-poly(propylene oxide)-*block*-poly(ethylene oxide) Inclusion Complexes

**Chi-Chun Tsai,[†] Siwei Leng,[†] Kwang-Un Jeong,[‡] Ryan M. Van Horn,[†] Chien-Lung Wang,[†] Wen-Bin Zhang,[†] Matthew J. Graham,[†] Jin Huang,[§] Rong-Ming Ho,[∥] Yongming Chen,*[,⊥] Bernard Lotz,*[,#] and Stephen Z. D. Cheng*[,†]**

[†]*Department of Polymer Science, College of Polymer Science and Polymer Engineering, University of Akron, Akron, Ohio 44325-3909, United States,* [‡]*Polymer BIN Fusion Research Center, Department of Polymer-Nano Science and Technology, Chonbuk National University, Jeonju, Jeonbuk 561-756, Korea,* [§]*College of Chemical Engineering, Wuhan University of Technology, Wuhan 430070, China,* [∥]*Department of Chemical Engineering, National Tsing Hua University, Hsinchu 30013, Taiwan,* [⊥]*State Key Laboratory of Polymer Physics and Chemistry, Institute of Chemistry, Chinese Academy of Science, Beijing 100190, China, and* [#]*Institut Charles Sadron, 23, Rue du Loess, Strasbourg 67034, France*

*Received August 22, 2010*

ABSTRACT: Supramolecular crystals were prepared via self-assembly of a series of inclusion complexes of β-cyclodextrin (β-CD) with poly(ethylene oxide)-*block*-poly(propylene oxide)-*block*-poly(ethylene oxide) (PEO-*b*-PPO-*b*-PEO) block copolymer. In this study, two PEO-*b*-PPO-*b*-PEO copolymers were used with different molecular weights for the PEO blocks. On the basis of two-dimensional (2D) wide-angle X-ray diffraction (WAXD) and selected area electron diffraction (SAED) experiments, the supramolecular crystal structure was determined to be a monoclinic lattice with $a = 1.910$ nm, $b = 2.426$ nm, $c = 1.568$ nm, and $\beta = 111°$ for both inclusion complex systems. Each crystal unit cell contained four inclusion complexes. The space group was identified to be $C_2$ symmetry based on the relationship among diffraction spot intensity and systematic extinctions. With the help of computer simulations of the supramolecular structure, the packing of inclusion complexes in the crystal lattice could be achieved. The simulated 2D WAXD fiber patterns and SAED patterns agreed well with the experimental results. Observations of the morphology in transmission electron microscopy combined with the [001] zone SAED patterns indicated that the supramolecular crystals are lozenge-shaped, bound by four (110) planes. Furthermore, the tethered PEO blocks were found to crystallize, and the *c*-axis of the PEO crystals was nearly parallel to the lamellar surface normal of the supramolecular crystals. The existence of PEO crystals resulted in additional proof that β-CDs are only selectively threaded onto the PPO blocks when forming the inclusion complexes. These PEO crystals acted as locks to prevent the dethreading of the β-CDs from the complexes and physically stabilized the supramolecular structure.

## Introduction

Molecular self-assembly, based on noncovalent interactions and molecular recognition, is a fascinating process that can be exploited to build up complex supramolecular structures.[1,2] Cyclodextrin (CD), one of the promising hosts for macromolecular recognition, has been studied for constructing supramolecular structures due to its good water solubility and ability to include a wide range of guest molecules.[3−6]

CDs are a series of cyclic oligosaccharides, containing 6, 7, or 8 glucose units connected through α-1,4-glycosidic linkages. They are abbreviated as α-, β-, and γ-CD, respectively. The shape of CDs is similar to a shallow, truncated cone that possesses a hydrophilic outer surface. At the primary (narrow-diameter end) and the secondary (wide-diameter end) rims of the molecule, there are hydroxyl groups. The central cavity consists of alkyl groups and glycosidic oxygen atoms and is hydrophobic. These CD cavities can thus act as a host for a variety of hydrophobic molecular guests.[7,8] It was suggested that a good accommodation between the cross-sectional area of a polymer chain and the minimum diameter size of the cyclodextrin cavity is the key to the formation of a stable polymer−CD inclusion complex.[5,6] The possibility of selective geometrical accommodation opens an interesting prospect when considering the complexation behavior of block copolymers with CDs. Recent studies have demonstrated that in inclusion complexes of CDs with block copolymers CDs can perform "site-selective complexation" on a specific segment of the block copolymer due to steric fitting, hydrophobic (or van der Waals) interaction, and/or other interactions between the cavity of CDs and the polymer, which can generate and/or enhance amphiphilicity of the block copolymers and further self-organize into supramolecular aggregates.[9−20] Furthermore, this self-assembled supramolecular structure can be manipulated by controlling temperature,[9,10] pH value,[16] and solvent type.[17,18] The tunable supramolecular structure through aggregation of inclusion complexes opens a great potential for applications in biomedical technologies[9,10,13,16,20] and nanoscience.[17−19]

The complexation behavior between poly(ethylene oxide)-*block*-poly(propylene oxide)-*block*-poly(ethylene oxide) (PEO-*b*-PPO-*b*-PEO) and β-CD has attracted great interests[21−27] since the complicated association and widespread utility of PEO-*b*-PPO-*b*-PEO, also

*To whom correspondence should be addressed. E-mail: ymchen@iccas.ac.cn (Y.C.), lotz@ics.u-strasbg.fr (B.L.), scheng@uakron.edu (S.Z.D.C.).

 Published on Web 10/20/2010 

**Scheme 1. Supramolecular Structure Formed via Hierarchical Self-Assembly Processes**

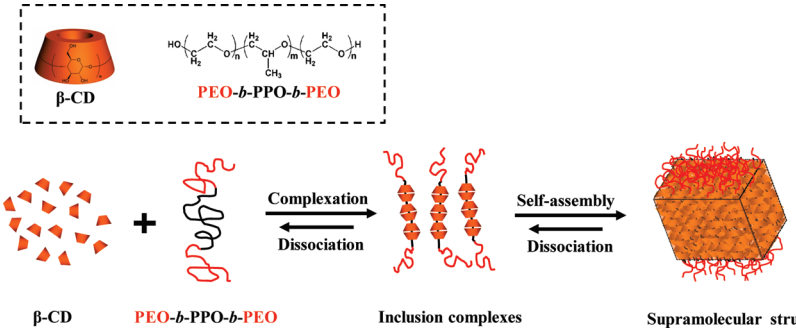


**Table 1. Molecular Characteristics of PEO-*b*-PPO-*b*-PEO Triblock Copolymers and *β*-CD Samples**

| sample | composition[a] | $\overline{M}_n$[b] (g/mol) | $\overline{M}_w/\overline{M}_n$[b] | PPO content[a] (wt %) |
|---|---|---|---|---|
| EPE77 | $EO_{64}PO_{37}EO_{64}$ | 7700 | ~1.2 | 27 |
| EPE146 | $EO_{137}PO_{44}EO_{137}$ | 14600 | ~1.2 | 17 |
| *β*-CD | $C_{42}H_{70}O_{35}$ | 1134 | | |

[a] Determined by $^1$H NMR. [b] Determined by GPC.

known as Pluronics, provide a good framework for the study of inclusion complexation behavior. Furthermore, the inclusion complexes are reversibly soluble and insoluble in response to temperature in aqueous solution. Therefore, it provides a robust model of stimuli-responsive supramolecules for nanoscale devices.[21,22] Recent studies in our group[28] have clarified the complexation behavior between PEO-*b*-PPO-*b*-PEO and *β*-CD utilizing solution and solid-state NMR experiments. The results indicated that the *β*-CDs possess selectivity on the PEO-*b*-PPO-*b*-PEO after complexation and only thread onto PPO blocks, not PEO blocks. However, the self-assembled supramolecular structure based on this inclusion complex has not been reported so far.

In this work, the supramolecular aggregate formed via self-assembly of inclusion complexes has been prepared, and the structure was determined, which is illustrated in Scheme 1. On the basis of wide-angle X-ray diffraction (WAXD), transmission electron microscopy (TEM), and computer simulation, the molecular packing in the supramolecular crystal structure can be built. The supramolecular structure exhibits a lozenge-shaped crystal morphology with {110} faces. Unlike less-ordered (or disordered) self-assembled aggregates such as micelles[14] and vesicles,[16] the supramolecular structure is constructed from a three-dimensionally well-defined crystal structure in aqueous solution. This hierarchical self-assembly of a well-ordered crystal structure provides one of the practical strategies to the development of "bottom-up" nanotechnology.

## Experimental Section

**Materials.** Two samples of PEO-*b*-PPO-*b*-PEO block copolymers with different molecular weights were purchased from Aldrich and were supplied as commercially available samples from BASF (EPE77 and EPE146). *β*-Cyclodextrin (*β*-CD) was purchased from Acros. All samples were used as received, and the molecular characteristics of PEO-*b*-PPO-*b*-PEO block copolymers and *β*-CD conducted using gel permeation chromatography (GPC) and $^1$H NMR are listed in Table 1.

**Preparation of Inclusion Complexes of PEO-*b*-PPO-*b*-PEO with *β*-CD.** An aqueous solution of *β*-CDs was mixed with an aqueous solution of copolymers in a molar ratio of *β*-CD/PO = 1:1 at room temperature. The temperature and concentration of the block copolymer solutions were controlled to be below the critical micellization concentration.[29] After mixing with *β*-CDs, solutions gradually became turbid and finally produced white precipitates, apparently indicating the formation of inclusion complexes. For TEM experiments, a drop of inclusion complex solution was pipetted onto a 400-mesh copper grid with a carbon-coated supporting film and washed with water twice. The samples were dried in a vacuum oven for 3 days at room temperature. The samples prepared for one-dimensional (1D) WAXD were vacuum-filtered with 0.4 *μ*m filter paper and washed with a limited amount of distilled water. After drying in vacuum at room temperature for 3 days, the bulk samples were gently ground into powder. To obtain an oriented supramolecular crystal for 2D WAXD experiments, the samples were prepared from the precipitated inclusion complex by slow sedimentation during filtration on the filter paper and dried in a vacuum oven at room temperature, again for 3 days. The same sample treatment procedure was followed to completely remove water from the samples. The abbreviations of the inclusion complexes between *β*-CD and the two copolymers are *β*-CD/EPE77 and *β*-CD/EPE146, respectively. The numerical portion represents the overall weight-average molecular weights of the triblock copolymers.

**Experiments and Measurements.** The thermal properties of the inclusion complexes were characterized with a Perkin-Elmer PYRIS Diamond DSC with an Intracooler 2P apparatus. The temperature and heat flow scales were calibrated at different heating and cooling rates (1−40 °C/min) using the standard materials. 1D WAXD patterns were obtained with a Rigaku Multiflex 2 kW automated diffractometer using Cu Kα radiation (0.1542 nm). The samples were scanned across a 2*θ* range of 2°−35° at a 1°/min scanning rate. The peak positions were calibrated using silicon powder in the high-angle region (>15°) and silver behenate in the low-angle region (<15°). For 2D WAXD patterns, a Rigaku 18 kW rotating anode X-ray generator attached to an R-AXIS-IV image plate system was used. The exposure time to obtain high-quality WAXD patterns was 45 min. The same standards were used to calibrate the 2*θ* angles. The crystal unit cells were determined by constructing reciprocal lattices. Computer refinement was conducted to find the solutions with the least error between the calculated values and the experimental results.[30−34] TEM experiments were carried out with a Philips Tecnai 12 using an accelerating voltage of 120 kV. Selected area electron diffraction (SAED) patterns were obtained using a TEM tilting stage to determine the crystal structure parameters. The *d*-spacings were calibrated using a TlCl standard. Computer molecular modeling and analysis of the diffraction patterns were performed using the Cerius$^2$ package of Accelrys. The lowest energy conformation of a pair of *β*-CDs included with two repeating units of propylene oxide was chosen as the starting conformation. Basic unit cell parameters determined by crystallographic experimental data from 2D WAXD and SAED experiments were used to build the crystal unit cell. The positions of atoms in this unit cell were judged by comparing their calculated diffraction patterns with those of experiments.

## Results and Discussion

**Identification of the Supramolecular Crystal Structure of Self-Assembled Inclusion Complexes.** Figure 1 exhibits a set

of 1D WAXD powder patterns observed for the self-assembled inclusion complexes, pure EPE77, and hydrated $\beta$-CD at room temperature in a $2\theta$ range from 3° to 35°. In the pure copolymer system, the PEO blocks crystallized to form a monoclinic structure with $a = 0.805$ nm, $b = 1.304$ nm, $c = 1.948$ nm, and $\beta = 125.4°$.[35] Therefore, in the WAXD of EPE77 (Figure 1a), there are two prominent reflection peaks at $2\theta = 19°$ assigned as the (120) reflection and at $2\theta = 23°$ which is attributed to several overlapped reflections.[36] The hydrated $\beta$-CD (Figure 1d) was reported to have a herringbone packing structure when it is complexed with water. Its crystal structure possesses a monoclinic unit cell with $a = 2.126$ nm, $b = 1.031$ nm, $c = 1.512$ nm, and $\beta = 112.3°$ with a space group of $P2_1$.[37] The diffraction patterns of the two self-assembled $\beta$-CD/EPE inclusion complexes shown in Figure 1b,c are quite different from the WAXD of the hydrated $\beta$-CD and pure copolymer. These differences indicate that the inclusion complexes form a different crystal structure. However, 1D WAXD powder patterns do not provide structural symmetry and unit cell lattices due to the lack of dimensionality of these reflections. Therefore, it is insufficient for complete structure determination. In order to accurately determine the supramolecular crystal structure of self-assembled inclusion complexes, a 2D WAXD fiber pattern from oriented crystals is required. The oriented single supramolecular crystal mats possess 2D WAXD fiber patterns as shown in Figure 2. These WAXD fiber patterns exhibit reflections not only on the equator and the meridian but also in quadrants (Figure 2a,b). After crystallographic analysis, it was found that the diffraction spots which are on the meridian in the low-angle region ($2\theta < 5°$) do not belong to the supramolecular crystal structure but are attributed to the alternating layers formed by stacking the supramolecular structures on top of each other during sedimentation (Figure 2), which indicates a uniformity in the size of the crystals along the drying direction. In addition, the diffraction pattern in Figure 2b also includes the PEO crystal diffraction and will be discussed later. At this moment, we exclude those diffractions attributed to the PEO crystal and alternating layers. For the inclusion complex crystals, we can identify that the $c$*-axis is on the meridian and that the $b$*-axis is on the equator, yet the $a$*-axis is 21° tilted away from the equator. Therefore, the (00$l$) planes are on the meridian and the (0$k$0) planes are on the equator. Using the reciprocal lattice method and refinement procedure,[30−34] the unit cell for the supramolecular crystal structure of $\beta$-CD/EPE77 (Figure 2a) is monoclinic with $a = 1.910$ nm, $b = 2.426$ nm, $c = 1.568$ nm, and $\beta = 111°$, and one crystal unit cell contains four inclusion complexes. The experimentally observed and calculated diffraction angles ($2\theta$) and $d$-spacing values of the crystal lattice are listed in Table 2. The space group is $C_2$ symmetry determined based on the relationships among diffraction spot intensities and the systematic extinctions. It is noteworthy that crystal structures for $\beta$-CD/EPE146 (Figure 2b) also show an almost identical monoclinic space group $C_2$ with $a = 1.900$ nm, $b = 2.435$ nm, $c = 1.570$ nm, and $\beta = 111°$ (see Table 3).

The supramolecular crystal structure can be further confirmed by the SAED experiments obtained from the supramolecular single crystal in TEM. Figure 3a shows an SAED pattern of the [103] zone, and the $c$*-axis of the single crystal is parallel to the electron beam, indicating the $ab$-plane of this crystal lies on the copper grid surface. On the basis of the determined monoclinic structure from 2D WAXD, the electron diffraction pattern with the [001] zone (Figure 3b) can be obtained by tilting clockwise 21° around the $b$*-axis. In Figure 3b, the odd-numbered diffraction spots on the (0$k$0) axis are extinct; therefore, the diffraction spots on the meridian that remain are the (020), (040), and (060) diffractions with a $d$-spacing of 1.21 nm between the neighboring (020) planes.

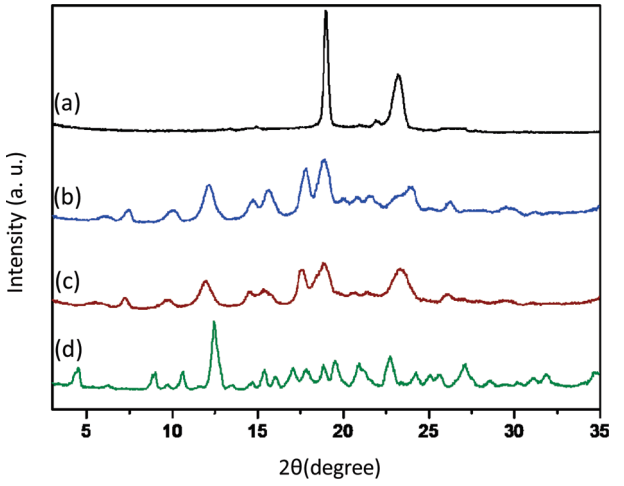


**Figure 1.** WAXD powder diffraction patterns for the EPE77 triblock copolymer (a), the $\beta$-CD/EPE77 inclusion complexes (b), the $\beta$-CD/EPE146 inclusion complexes (c), and the hydrated $\beta$-CD (d).

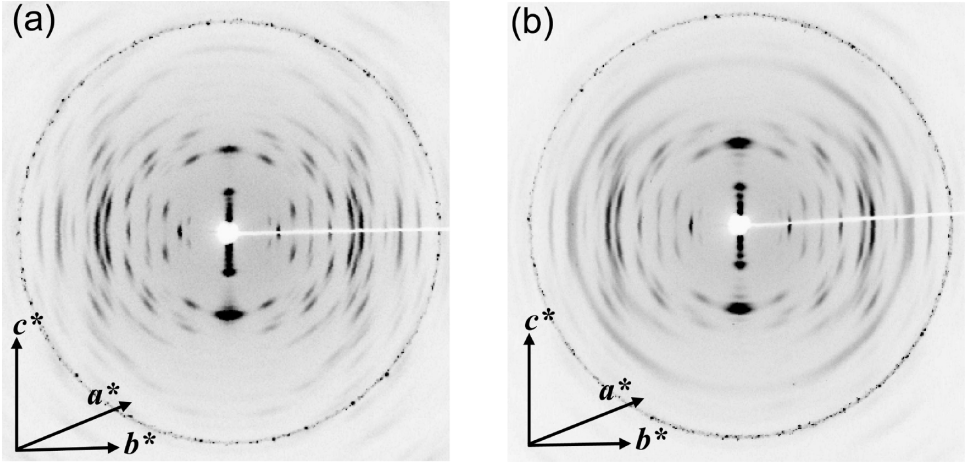


**Figure 2.** 2D WAXD fiber diffraction patterns for the supramolecular structure of the $\beta$-CD/EPE77 inclusion complexes (a) and the $\beta$-CD/EPE146 inclusion complexes (b). The ring diffraction pattern at $2\theta = 28.46°$ is attributed to standard sample of silicon powder.

**Table 2. Crystallographic Parameters of Supramolecular Structure of β-CD/EPE77 Inclusion Complexes**

| | | 2θ (deg) | | d-spacing (nm) | |
|---|---|---|---|---|---|
| no. | *hkl* | exptl[a] | calc[b] | exptl[a] | calc[b] |
| 1 | (001) | 6.03 | 6.03 | 1.46 | 1.46 |
| 2 | (110) | 6.15 | 6.15 | 1.44 | 1.44 |
| 3 | (020) | 7.28 | 7.28 | 1.21 | 1.21 |
| 4 | $(20\bar{1})$ | 9.62 | 9.59 | 0.92 | 0.92 |
| 5 | (200) | 9.92 | 9.92 | 0.89 | 0.89 |
| 6 | $(11\bar{2})$ | 11.9 | 11.8 | 0.74 | 0.75 |
| 7 | (130) | 12.0 | 12.0 | 0.74 | 0.74 |
| 8 | (002) | 12.1 | 12.1 | 0.73 | 0.73 |
| 9 | $(20\bar{2})$ | 12.5 | 12.6 | 0.71 | 0.70 |
| 10 | $(13\bar{1})$ | 12.6 | 12.6 | 0.70 | 0.70 |
| 11 | (201) | 13.5 | 13.4 | 0.66 | 0.66 |
| 12 | (022) | 14.1 | 14.1 | 0.63 | 0.63 |
| 13 | (040) | 14.6 | 14.6 | 0.61 | 0.61 |
| 14 | $(22\bar{2})$ | 14.6 | 14.6 | 0.61 | 0.61 |
| 15 | (112) | 15.1 | 15.1 | 0.59 | 0.59 |
| 16 | (310) | 15.4 | 15.3 | 0.58 | 0.58 |
| 17 | $(13\bar{2})$ | 15.7 | 15.7 | 0.56 | 0.56 |
| 18 | (041) | 15.8 | 15.8 | 0.56 | 0.56 |
| 19 | (240) | 17.7 | 17.7 | 0.50 | 0.50 |
| 20 | (202) | 18.2 | 18.2 | 0.49 | 0.49 |
| 21 | (132) | 18.3 | 18.3 | 0.49 | 0.49 |
| 22 | (311) | 18.5 | 18.4 | 0.48 | 0.48 |
| 23 | (330) | 18.6 | 18.5 | 0.48 | 0.48 |
| 24 | (150) | 18.9 | 18.9 | 0.47 | 0.47 |
| 25 | (241) | 19.9 | 19.8 | 0.45 | 0.45 |
| 26 | $(42\bar{2})$ | 20.7 | 20.6 | 0.43 | 0.43 |
| 27 | $(15\bar{2})$ | 21.5 | 21.5 | 0.41 | 0.41 |
| 28 | (060) | 21.9 | 21.9 | 0.41 | 0.41 |
| 29 | (260) | 23.8 | 24.1 | 0.37 | 0.37 |
| 30 | (170) | 26.0 | 26.2 | 0.34 | 0.34 |

[a] Experimental values observed in Figure 2a. [b] Calculated based on the monoclinic unit cell of $a = 1.910$ nm, $b = 2.426$ nm, $c = 1.568$ nm, $\alpha = 90°$, $\gamma = 90°$, and $\beta = 111°$.

Along the $a^*$-axis, a pair of weak diffraction spots with a $d$-spacing of 0.95 nm is assigned as the (200) diffraction since the odd-numbered diffraction spots are also extinct. The $\gamma^*$ angle between the $a^*$- and $b^*$-axes is 90°, which is consistent with the $\gamma$-angle calculated based on the 2D WAXD results. The 2D unit cell assignment of the $ab$-plane is, therefore, found to agree well with the structure determined via the 2D WAXD experiments (as shown in Figure 2).

From the results of the 2D WAXD fiber patterns and SAED patterns, the supramolecular single crystal structure obtained from another PEO-*b*-PPO-*b*-PEO copolymer with β-CD (β-CD/EPE146) also possesses the identical crystal structure as analyzed for β-CD/EPE77 in Figures 2 and 3. On the basis of our previous studies provided from the nuclear magnetic resonance results,[28] the threaded β-CD molecules in both of these systems are located around the PPO blocks. The only difference is the molecular weights of the PEO blocks are different in these two systems. Therefore, we can conclude that in these supramolecular single crystals the PPO blocks with threaded β-CDs are the building blocks, and they are closely packed to form the lamellar single crystals. The PEO blocks are attached to the lamellar crystal surfaces, acting as tethered chain molecules. Only closely packed supramolecular single crystals having long-range order can exhibit diffractions in WAXD and SAED patterns (Figures 2 and 3).

**Crystallographic Simulation of Molecular Packing.** The supramolecular building block packing in the single crystal can be verified via computer calculation. To build up this structure with four inclusion complexes with the $C_2$ space group, basic unit cell parameters according to the experimental data deduced from the 2D WAXD and SAED results are used. Since the tethered PEO blocks do not take part in the supramolecular single crystals, we excluded them in this computer calculation. Only the PPO blocks and threaded β-CDs are involved in this simulation. Figure 4 presents a series of the supramolecular building block packing schemes along different zones. These schemes are used to generate the calculated 2D WAXD fiber pattern and the [001] zone SAED pattern as shown in Figure 5a,b, which are the best fits with the experimental results. The computer simulation shown in Figure 4 reveals that one threaded β-CD on the PPO polymer chain occupies two chemical repeating units of PPO, since one β-CD possesses a height of 0.75 nm and two chemical repeating units of PPO is 0.71 nm in its free energy minimized conformation of an extended PPO chain. Furthermore, as shown in Figure 4a, the β-CDs are suggested to be in a tail-to-tail arrangement along the extended PPO chain (the $c$-axis in the crystal) to form a 1D column as the building block to construct the supramolecular single crystals. This type of columnar building block has been frequently observed in the cases when β-CDs formed channel-type inclusion complexes with guest molecules.[38−45] In the columnar building blocks, β-CDs tend to arrange into the thermodynamically most stable tail-to-tail dimers (a motif of the column) because in such a dimer arrangement the inter-β-CD hydrogen bonds between the secondary hydroxyls are preferentially formed. However, β-CDs are not stacked in a straight line when viewing along the $b$-axis but, rather, form an inclined column as shown in Figure 4a. The explanation for the inclined column structure could be attributed to a cooperation of interactions resulting from hydrogen bonding between β-CDs as well as spatial fitting between β-CDs and the atactic PPO chain. Note that the atactic PPO chain does not possess a conformational regularity and that it is selectively included in the inner cavity of β-CDs. The overall PPO block conformation in the single crystals is a balance between the need to minimize intramolecular steric interaction of the PPO itself and space filling the β-CD cavity by maximizing the PPO−β-CD physical interactions. The distance between β-CD and

**Table 3. Crystallographic Parameters of Supramolecular Structure of β-CD/EPE146 Inclusion Complexes**

| | | 2θ (deg) | | d-spacing (nm) | |
|---|---|---|---|---|---|
| no. | *hkl* | exptl[a] | calc[b] | exptl[a] | calc[b] |
| 1 | (001) | 6.03 | 6.03 | 1.466 | 1.466 |
| 2 | (110) | 6.16 | 6.16 | 1.434 | 1.434 |
| 3 | (020) | 7.26 | 7.26 | 1.22 | 1.22 |
| 4 | $(20\bar{1})$ | 9.65 | 9.63 | 0.92 | 0.92 |
| 5 | (200) | 9.97 | 9.97 | 0.89 | 0.89 |
| 6 | $(11\bar{2})$ | 11.9 | 11.8 | 0.74 | 0.75 |
| 7 | (130) | 12.0 | 12.0 | 0.74 | 0.74 |
| 8 | (002) | 12.1 | 12.1 | 0.73 | 0.73 |
| 9 | $(13\bar{1})$ | 12.6 | 12.6 | 0.70 | 0.70 |
| 10 | (022) | 14.1 | 14.1 | 0.63 | 0.63 |
| 11 | (040) | 14.5 | 14.5 | 0.61 | 0.61 |
| 12 | $(22\bar{2})$ | 14.6 | 14.6 | 0.61 | 0.61 |
| 13 | (112) | 15.0 | 15.1 | 0.59 | 0.59 |
| 14 | (310) | 15.4 | 15.4 | 0.57 | 0.57 |
| 15 | $(13\bar{2})$ | 15.7 | 15.7 | 0.56 | 0.56 |
| 16 | (240) | 17.6 | 17.6 | 0.50 | 0.50 |
| 17 | (330) | 18.6 | 18.6 | 0.48 | 0.48 |
| 18 | (150) | 18.9 | 18.9 | 0.47 | 0.47 |
| 19 | (241) | 19.9 | 19.8 | 0.45 | 0.45 |
| 20 | $(42\bar{2})$ | 20.6 | 20.6 | 0.43 | 0.43 |
| 21 | $(15\bar{2})$ | 21.5 | 21.4 | 0.41 | 0.41 |
| 22 | (060) | 21.9 | 21.9 | 0.41 | 0.41 |
| 23 | (260) | 24.2 | 24.1 | 0.37 | 0.37 |
| 24 | (170) | 26.1 | 26.1 | 0.34 | 0.34 |

[a] Experimental values observed in Figure 2b. [b] Calculated based on the monoclinic unit cell of $a = 1.900$ nm, $b = 2.435$ nm, $c = 1.570$ nm, $\alpha = 90°$, $\gamma = 90°$, and $\beta = 111°$.

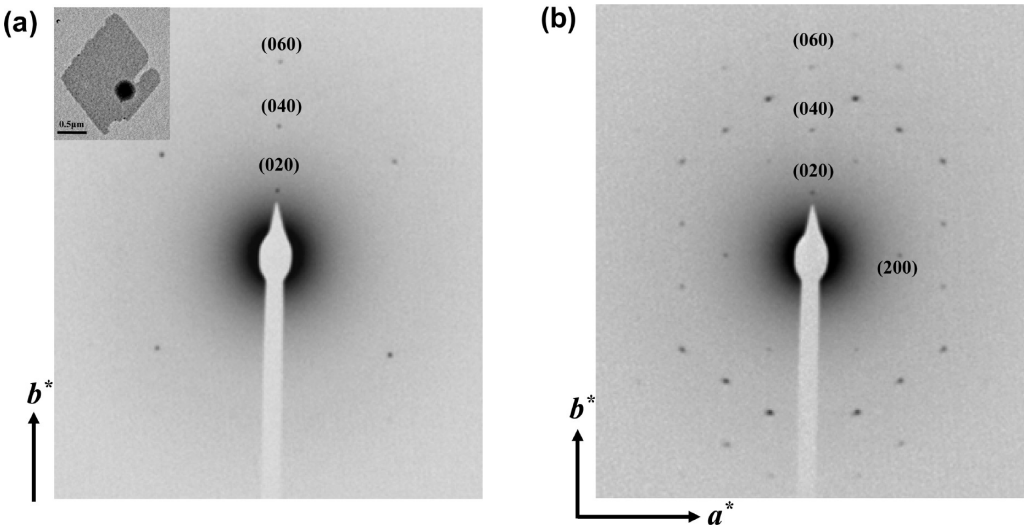


**Figure 3.** TEM bright field morphology (inset image) and SAED of the [103] zone for the single supramolecular crystal of $\beta$-CD/EPE77 inclusion complexes (a) and the [001] zone (b). The pattern of (b) was obtained by tilting 21° around the $b^*$-axis from pattern (a).

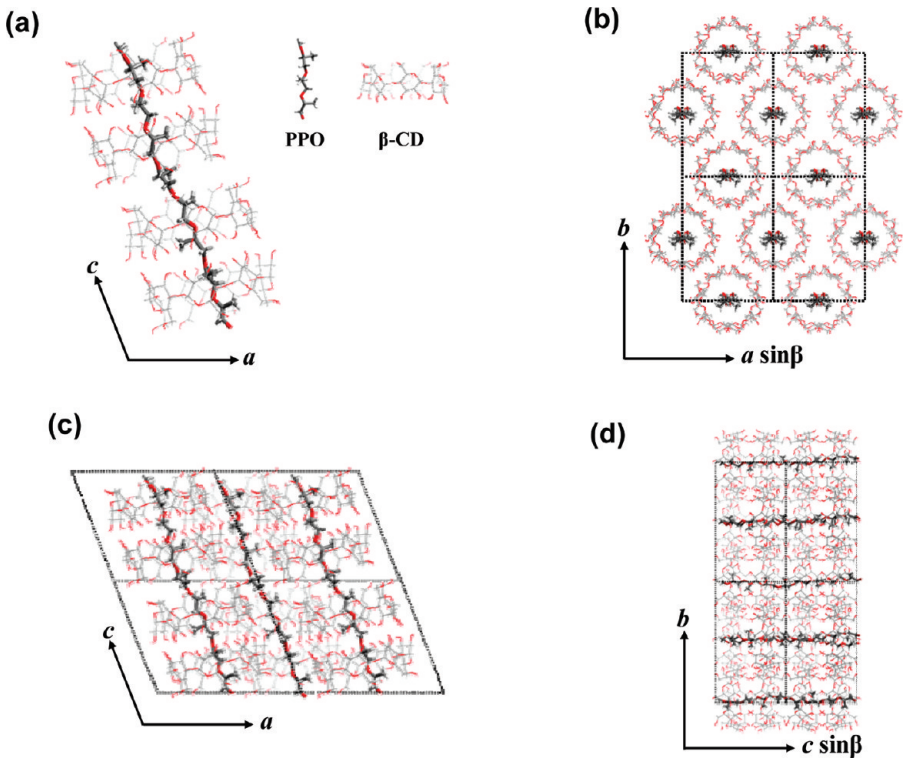


**Figure 4.** Molecular packing schemes based on computer simulation. The channel-type structure composed of four symmetric related inclusion complexes viewed along the *b*-axis (a), the molecular packing in the crystal lattice viewed along the [001] zone (b), viewed along the [010] zone (c), and viewed along the [100] zone. The molecular packing schemes of (b), (c), and (d) contain four unit cells along each projection plane.

PPO has been investigated to be less than 0.4 nm evidenced by 2D ROESY experimental results as reported in our previous study.[28] The conformation of the PPO chain contains both *trans* and *gauche* configurations. As a result, the PPO chain is disordered within the cavity of $\beta$-CDs and does not contribute to the crystallographic symmetry.

On the basis of quantitative analysis of the 2D WAXD fiber patterns as shown in Figure 2, it is observed that the intensity of the diffraction for the (002) spot is stronger than that of the (001) spot. In addition, the diffraction spots of the (150), (240), (13$\bar{2}$), (11$\bar{2}$), (310), and (330) planes also possess strong diffraction intensities. From the computed packing scheme in the crystal lattice, it has been determined that the (002) planes are located on the secondary hydroxyls of the $\beta$-CDs compared with the (001) planes. Only the primary hydroxyl groups are located on the (001) planes. Therefore, the (002) plane possesses a higher number of atoms and thus contributes to a stronger electron density. On the other hand, the stronger intensities on the (150), (240), (13$\bar{2}$), (11$\bar{2}$), (310), and (330) diffractions are due to the fact that the hydroxyl groups and/or the glycosidic oxygen atoms of $\beta$-CD are largely located on these planes.

**Crystal Morphology of Supramolecular Structure of Inclusion Complexes.** Figure 6a shows a supramolecular single crystal morphology observed in TEM and its corresponding

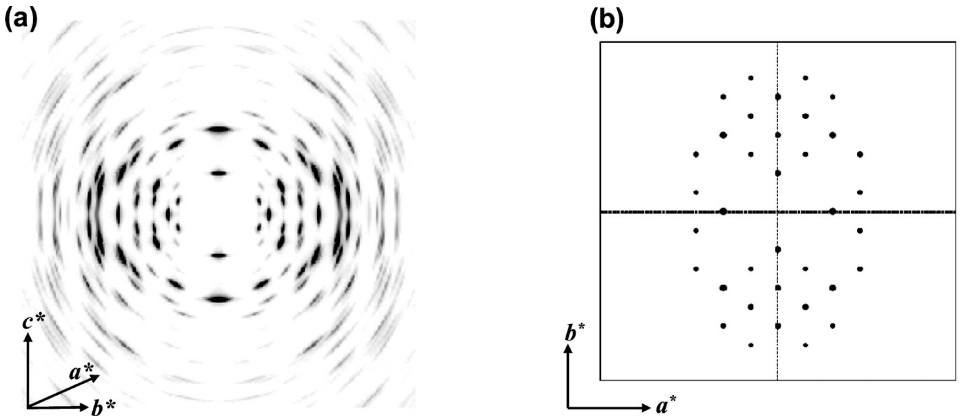


**Figure 5.** Computer calculated 2D WAXD fiber pattern (a) and SAED pattern of the [001] zone (b) which is the best fits with the experimental 2D WAXD (Figure 2) and SAED diffraction patterns (Figure 3b).

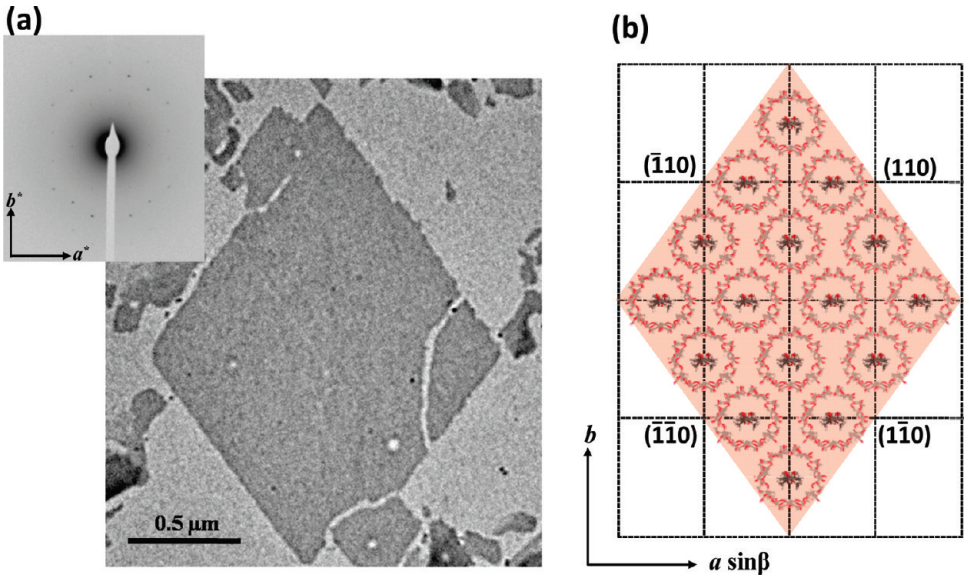


**Figure 6.** TEM bright field morphology image and SAED pattern of the [001] zone (inset) for a single supramolecular crystal of $\beta$-CD/EPE77 inclusion complexes (a) and the resultant crystal morphology based on computer simulation (b).

SAED pattern from the [001] zone. The observed morphology under TEM was lozenge-shaped. On the basis of the [001] zone SAED pattern, the $b$*-axis points toward the acute angle, while the $a$*-axis is toward the obtuse angle with respect to this crystal morphology. The acute angle is estimated to be ~73°, which matches the acute angle between the (110) and the ($\bar{1}$10) planes calculated based on the computer simulation (Figure 6b). Therefore, the observed lozenge-shaped supramolecular single crystal is bounded by four (110) planes. From the crystallographic point of view, for a monoclinic unit cell with $\beta = 111°$ to construct a lozenge-shaped single crystal, the necessary condition is that this single crystal must align the long axis of this columnar building block parallel to the $c$-axis as shown in the computer simulation (Figure 4a) and a flat crystal surface that is parallel to the $a$*$b$-plane (Figure 4b). Note that the size of the supramolecular single crystal along the $c$-axis (Figure 4c) is limited by the length of the PPO block that can accommodate the threaded $\beta$-CDs along the chain direction.[46,47] Furthermore, the existence of the PEO blocks as tethered chains on both sides of the single crystal surfaces does not allow crystal development along the [001] direction. Hence, the supramolecular crystal can only grow along $a$*- and $b$-axes, resulting in the lozenge-shaped lamellar single crystal morphology (Figure 6a).

**Crystallization Behavior and Crystal Orientation of PEO Blocks on the Supramolecular Crystal.** The structure of PEO crystals has been well-studied and is commonly observed as a monoclinic unit cell, formed from a helical conformation, with $a = 0.805$ nm, $b = 1.304$ nm, $c = 1.948$ nm, and $\beta = 125.4°$.[35,36,48−54] The PEO single crystal is a flat platelet with the $c$-axis normal to the basal surface, which means the basal plane is close to the (10$\bar{4}$) with a squarelike shape bound by four (120) planes. Therefore, the PEO single crystal grows parallel to the $a$*$b$-plane.[49−52] In our supramolecular complex systems, the molecular weights of the PEO blocks are high enough to crystallize at room temperature.[53,54] On the basis of our differential scanning calorimetric study, the crystallinity of the PEO blocks in $\beta$-CD/EPE77 is only about 6%. They do not provide strong crystal diffraction in the 2D WAXD pattern as shown in Figure 2a. Nevertheless, the PEO blocks in $\beta$-CD/EPE146 can possess a crystallinity up to 21%. Therefore, the PEO crystal diffraction must be included in the 2D WAXD pattern as shown in Figure 2b. This provides an opportunity to investigate the crystal orientation of the PEO blocks after they have crystallized on the supramolecular single crystals. To remove previous thermal history during water evaporation, the samples are heated to 80 °C to melt all the PEO crystals and subsequently cooled to

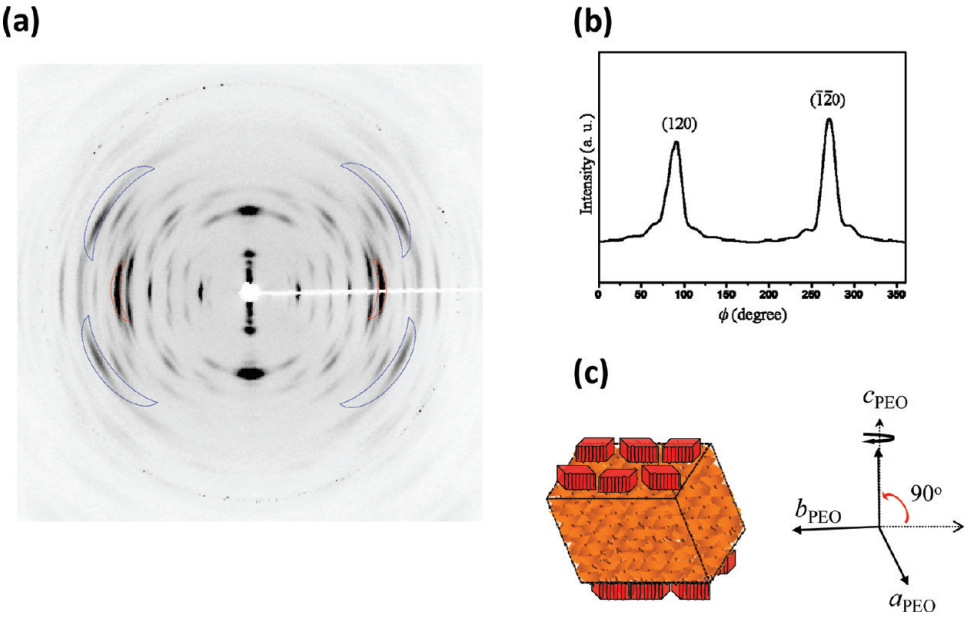


**Figure 7.** 2D WAXD fiber diffraction patterns for supramolecular structure of $\beta$-CD/EPE146 inclusion complexes (a), azimuthal profile of the (120) diffractions of PEO crystals (b), and schematic of PEO crystal orientation on the supramolecular structure (c).

room temperature. Compared with 2D WAXD fiber patterns of $\beta$-CD/EPE77 (Figure 2a), the PEO crystal diffractions in the 2D WAXD fiber patterns of $\beta$-CD/EPE146 can be identified, and they are indicated by red and blue circles as shown in Figure 7a. The red circle marked diffractions are attributed to the (120) planes at $2\theta = 19°$ ($d$-spacing = 0.463 nm), while the blue circle marked diffractions at $2\theta = 23°$ ($d$-spacing = 0.390 nm) belong to the mixed diffractions of the ($\bar{1}32$), (032), ($\bar{2}12$), (112), ($\bar{1}24$), ($\bar{2}04$), and (004).[35,36] The azimuthal profile for first ring of (120) diffractions is shown in Figure 7b, and the (120) planes are at $\phi = 90°$ and 270°. On the basis of the 2D WAXD experiments, it was found that the $c$-axis of the PEO crystal is parallel to the basal surface normal of the supramolecular single crystal (the $a^*b$-plane of the supramolecular lattice), as schematically illustrated in Figure 7c. Furthermore, we have carried out several isothermal crystallization experiments for these PEO blocks in a wide temperature region from −20 to 30 °C; no PEO crystal orientation change was observed. Therefore, it is concluded that the nano-confinement in this case must be different from the PEO confined crystallization between polystyrene layers in the diblock copolymers.[55−57]

The observation of the PEO crystals on the surface of the supramolecular single crystals is also indicative that the $\beta$-CDs are selectively threaded onto the PPO blocks. Furthermore, the PEO crystals now form "locks" for the $\beta$-CDs to not allow them to escape from the supramolecular single crystals. The results indicate that stable and well-ordered supramolecular single crystals can be constructed through self-assembly of inclusion complexes in aqueous solution, which provides a new approach for built-up nanostructures via hierarchical self-assembly processes.

## Conclusions

In summary, supramolecular crystal structures are formed via self-assembly of a series of $\beta$-CD/PEO-$b$-PPO-$b$-PEO inclusion complexes. On the basis of 2D WAXD fiber patterns and SAED patterns, the crystal structure was determined to be monoclinic with $a = 1.906$ nm, $b = 2.430$ nm, $c = 1.572$ nm, and $\beta = 111°$ for all the inclusion complex systems studied. Each crystal unit cell contains four inclusion complex building blocks. The space group is $C_2$ determined based on the relationship among diffraction spot intensity and systematic extinctions. Through computer simulation of supramolecular structure utilizing the Cerius[2] software, the packing of inclusion complexes in the crystal lattice was investigated. The simulated 2D WAXD fiber patterns and SAED patterns agreed well with experimental results. The observation of crystal morphology from TEM and combined with [001] zone SAED patterns indicates that the supramolecular crystal structures are lozenge-shaped and bound by four (110) planes. Furthermore, the 2D WAXD experiment results revealed that the tethered PEO blocks can crystallize on the supramolecular crystals when their molecular weights are high enough. The $c$-axis of the PEO crystals is oriented parallel to the basal surface normal of the supramolecular crystal. The finding of PEO block crystals on the supramolecular structure provides additional proof that $\beta$-CDs only selectively thread onto the PPO block when forming inclusion complexes.

**Acknowledgment.** This work was supported by NSF (DMR-0906898).

## References and Notes

(1) Lehn, J. M. *Supramolecular Chemistry: Concepts and Perspectives*; VCH: Weinheim, 1995.
(2) Steed, J. W.; Atwood, J. L. *Supramolecular Chemistry*; John Wiley & Sons: New York, 2000.
(3) Harada, A. *Coord. Chem. Rev.* **1996**, *148*, 115.
(4) Herrmann, W.; Keller, B.; Wenz, G. *Macromolecules* **1997**, *30*, 4966.
(5) Harada, A.; Li, J.; Kamachi, M. *Polym. Adv. Technol.* **1997**, *8*, 241.
(6) Harada, A.; Okada, M.; Kawaguchi, Y.; Kamachi, M. *Polym. Adv. Technol.* **1999**, *10*, 3.
(7) Wenz, G. *Angew. Chem., Int. Ed. Engl.* **1994**, *33*, 803.
(8) Szejtli, J. *Cyclodextrins and Their Inclusion Complexes*; Akademiai Kiado: Budapest, 1982.
(9) Li, J.; Li, X.; Zhou, Z.; Ni, X.; Leong, K. W. *Macromolecules* **2001**, *34*, 7236.
(10) Huh, K. M.; Ooya, T.; Lee, W. K.; Sasaki, S.; Kwon, I. C.; Jeong, S. Y.; Yui, N. *Macromolecules* **2001**, *34*, 8657.
(11) Sabadini, E.; Cosgrove, T. *Langmuir* **2003**, *19*, 9680.
(12) Li, J.; Ni, X.; Zhou, Z.; Leong, K. W. *J. Am. Chem. Soc.* **2003**, *125*, 1788.
(13) He, L.; Huang, J.; Chen, Y.; Xu, X.; Liu, L. *Macromolecules* **2005**, *38*, 3845.

(14) Huang, J.; Ren, L.; Zhu, H.; Chen, Y. M. *Macromol. Chem. Phys.* **2006**, *207*, 1764.
(15) Wenz, G.; Han, B. H.; Muller, A. *Chem. Rev.* **2006**, *106*, 782.
(16) Liu, J.; Sondjaja, H. R.; Tam, K. C. *Langmuir* **2007**, *23*, 5106.
(17) Chung, J. W.; Kang, T. J.; Kwak, S. Y. *Macromolecules* **2007**, 4225.
(18) Ren, L.; Ke, F.; Chen, Y.; Liang, D.; Huang, J. *Macromolecules* **2008**, *41*, 5295.
(19) Yang, C.; Wang, X.; Li, H.; Ding, J. L.; Wang, D. Y.; Li, J. *Polymer* **2009**, *50*, 1378.
(20) Tu, C. W.; Kuo, S. W.; Chang, F. C. *Polymer* **2009**, *50*, 2985.
(21) Fujita, H.; Ooya, T.; Kurisawa, M.; Mori, H.; Terano, M.; Yui, N. *Macromol. Rapid Commun.* **1996**, *17*, 509.
(22) Fujita, H.; Ooya, T.; Yui, N. *Macromolecules* **1999**, *32*, 2534.
(23) Mayera, B.; Kleina, C. T.; Topchieva, I. N.; Kohlera, G. *J. Comput.-Aided Mol. Des.* **1999**, *13*, 373.
(24) Topchieva, I. N.; Kolomnikova, E. L.; Banatskaya, M. I.; Kabanov, V. A. *Polym. Sci.* **1993**, *35*, 464.
(25) Topchieva, I. N.; Blyumenfeld, A. L.; Klyamkin, A. A.; Polyakov, V. A.; Kabanov, V. A. *Polym. Sci.* **1994**, *36*, 221.
(26) Panova, I. G.; Gerasimov, V. I.; Tashlitskii, V. N.; Topchieva, I. N.; Kabanov, V. A. *Polym. Sci., Ser. A* **1997**, *39*, 452.
(27) Topchieva, I. N.; Gerasimov, V. I.; Panova, I. G.; Karezin, K. I.; Efremova, N. V. *Polym. Sci., Ser. A* **1998**, *40*, 171.
(28) Tsai, C.-C.; Zhang, W. B.; Wang, C. L.; Van Horn, R. M.; Graham, M. J.; Huang, J.; Chen, Y.; Guo, M.; Cheng, S. Z. D. *J. Chem. Phys.* **2010**, *132*, 204903.
(29) Alexandridis, P.; Holzwarth, J. F.; Hatton, T. A. *Macromolecules* **1994**, *27*, 2414.
(30) Cheng, S. Z. D.; Wu, Z.; Eashoo, M.; Hsu, S. L.; Harris, F. W. *Polymer* **1991**, *32*, 1803.
(31) Eashoo, M.; Wu, Z.; Zhang, A.; Shen, D.; Tse, C.; Harris, F. W.; Cheng, S. Z. D.; Gardner, K. H.; Hsiao, B. S. *Macromol. Chem. Phys.* **1994**, *195*, 2207.
(32) Ge, J. J.; Zhang, A.; McCreight, K. W.; Ho, R. M.; Wang, S. Y.; Jin, X.; Harris, F. W.; Cheng, S. Z. D. *Macromolecules* **1997**, *30*, 6498.
(33) Jing, A. J.; Taikum, O.; Li, C. Y.; Harris, F. W.; Cheng, S. Z. D. *Polymer* **2002**, *43*, 3431.
(34) Ruan, J.; Ge, J. J.; Zhang, A.; Shi, J.; Wang, S. Y.; Harris, F. W.; Cheng, S. Z. D. *Macromolecules* **2002**, *35*, 736.
(35) Takahashi, Y.; Tadokoro, H. *Macromolecules* **1973**, *6*, 672.
(36) Zhu, L.; Cheng, S. Z. D.; Calhoun, B. H.; Ge, Q.; Quirk, R. P.; Thomas, E. L.; Hsiao, B. S.; Yeh, F.; Lotz, B. *J. Am. Chem. Soc.* **2000**, *122*, 5957.
(37) Betzel, C.; Saenger, W.; Hingerty, B. E.; Brown, G. M. *J. Am. Chem. Soc.* **1984**, *106*, 7545.
(38) Mentzafos, D.; Mavridis, I. M.; Le Bas, G.; Tsoucaris, G. *Acta Crystallogr., Sect. B* **1991**, *47*, 746.
(39) Udachin, K. A.; Ripmeester, J. A. *J. Am. Chem. Soc.* **1998**, *120*, 1080.
(40) Kamitori, S.; Matsuzaka, O.; Kondo, S.; Muraoka, S.; Okuyama, K.; Noguchi, K.; Okada, M.; Harada, A. *Macromolecules* **2000**, *33*, 1500.
(41) Aree, T.; Chaichi, N. *Carbohydr. Res.* **2003**, *338*, 439.
(42) Aree, T.; Chaichi, N. *Carbohydr. Res.* **2003**, *338*, 1581.
(43) Takashima, Y.; Oizumi, Y.; Sakamoto, K.; Miyauchi, M.; Kamitori, S.; Harada, A. *Macromolecules* **2004**, *37*, 3962.
(44) Kokkinou, A.; Makedonopoulou, S.; Mentzafos, D. *Carbohydr. Res.* **2000**, *328*, 135.
(45) Kokkinou, A.; Yannakopoulou, K.; Mavridis, I. M.; Mentzafo, D. *Carbohydr. Res.* **2001**, *332*, 85.
(46) Harada, A.; Okada, M.; Li, J.; Kamachi, M. *Macromolecules* **1995**, *28*, 8406.
(47) Harada, A.; Okada, M.; Kamachi, M. *Acta Polym.* **1995**, *46*, 453.
(48) Tadokoro, H.; Chatani, Y.; Yoshihara, T.; Tahara, S.; Murahashi, S. *Makromol. Chem.* **1964**, *73*, 109.
(49) Lotz, B.; Kovacs, A. J. *Kolloid Z. Z. Polym.* **1966**, *209*, 97.
(50) Lotz, B.; Kovacs, A. J.; Bassett, G. A.; Keller, A. *Kolloid Z. Z. Polym.* **1966**, *209*, 115.
(51) Kovacs, A. J.; Lotz, B.; Keller, A. J. *Macromol. Sci. Phys.* **1969**, *B3* (3), 385.
(52) Chen, J.; Cheng, S. Z. D.; Wu, S. S.; Lotz, B.; Wittmann, J. C. *J. Polym. Sci., Polym. Phys. Ed.* **1995**, *33*, 1851.
(53) Cheng, S. Z. D.; Wunderlich, B. *J. Polym. Sci., Part B* **1986**, *24*, 577.
(54) Cheng, S. Z. D.; Wunderlick, B. *J. Polym. Sci., Part B* **1986**, *24*, 595.
(55) Huang, P.; Zhu, L.; Guo, Y.; Ge, Q.; Jing, A. J.; Chen, W. Y.; Quirk, R. P.; Cheng, S. Z. D.; Thomas, E. L.; Lotz, B.; Hsiao, B. S.; Carlos, A.-O. A.; Sics, I. *Macromolecules* **2004**, *37*, 3689.
(56) Hsiao, M.-S.; Zheng, J. X.; Leng, S.; Van Horn, R. M.; Quirk, R. P.; Thomas, E. L.; Chen, H.-L.; Hsiao, B. S.; Rong, L.; Lotz, B.; Cheng, S. Z. D. *Macromolecules* **2008**, *41*, 8114.
(57) Hsiao, M.-S.; Zheng, J. X.; Van Horn, R. M.; Quirk, R. P.; Thomas, E. L.; Chen, H.-L.; Bernard Lotz, B.; Cheng, S. Z. D. *Macromolecules* **2009**, *42*, 8343.